

Design of A Wideband Compact Electromagnetic Band Gap Structure for Lower Frequency Applications

Abstract. A compact planar design of EBG structure with wide band gap is proposed in this study. The characteristic of the initial JC-EBG shape is analyzed by varying different dimensions and later improved results are obtained with a modified design. The maximum band gap achieved is 3.1 GHz (1.75-4.85 GHz), which is 31.91% more than initial one (2.35 GHz) and the lowest level of transmission coefficient obtained is around -100dB, with 12.5 mm unit cell size. The structure is designed on easily available standard PCB material and exhibits good performance in lower frequency range (below 6 GHz). Analyzed results showed the compatibility and tunability of the design for applications like GSM, PCS, WiMax, UMTS, WiFi, and Bluetooth etc.

Streszczenie. W artykule opisano projekt tloczonej powierzchniowo struktury materiału EBG z szeroką przerwą energetyczną. Analizie poddano charakterystykę kształtu JC-EBG, poprzez wprowadzenie zmienności poszczególnych wymiarów. Proponowana struktura została opracowana na standardowym materiale PCB. Wykazuje dobre właściwości w zakresie częstotliwości poniżej 6GHz. Wyniki analizy pokazują możliwość szerokiego zastosowania opisanego rozwiązania. (Projekt powierzchniowo tloczonej struktury EBG w aplikacji do niższych częstotliwości).

Keywords: compact, band gap, wideband, EBG, high impedance surfaces.

Słowa kluczowe: tloczenie, przerwa energetyczna, szerokopasmowy, EBG, podłoże wysoko-impedancyjne;

Introduction

The advancement and rapid growth in the technology boosted up the demand of compact and high speed devices for versatile applications [1,2,3]. Design of compact portable wireless devices with enhanced performance is an optimal challenge, where various radiating devices can be arranged in close proximity. In a compact integrated system like antenna array, the scope of mutual coupling, surface wave loss, noise increases and in progression it adversely affects the total functional efficiency of the system [4,6,9]. Recently, electromagnetic bandgap (EBG) structures were introduced as an effective alternative solution against these shortcomings [5,7,8,9,10]. The EBG structures are periodic arrangement of metallic or dielectric elements that provides high impedance surface, shows the ability to suppress the surface waves, control and guide the electromagnetic wave efficiently. Integration of EBG structure can improve the efficiency of printed circuits and antennas [10,11,12].

In the early phases, three dimensional periodic structures in different formations were studied extensively. But the design and fabrication complexities related to those configurations inspired researchers in designing planar EBG such as mushroom-like, fork-like and uni-planar EBG (UCEBG) etc. [5,9,13,14,16]. The UCEBG structures are simpler than the other forms in the way of exemption of grounding via. Some planar designs of EBG have been reported in the literature showed a stop band (or surface wave band gap) at or higher than 6 GHz [15,16,17,18]. However, considering the need to cope with a wide range of applications in the lower bands compact uni-planar type EBG structures are much more desirable. Authors in [19] proposed a planar configuration with 920 mils (23.37 mm) square-shape unit cell designed on a high permittivity substrate materials for lower bands. The band gap obtained is 1 GHz (2.5 to 3.5 GHz) but still there are scopes to consider the size issues. The multilayer design proposed in [20] for mobile phone applications, consists of 16.7x 3 mm² unit cell, exhibits a band gap of 0.24 GHz. Conversely, wide band gap at lower frequencies can be achieved with larger unit cells but it will not be cost effective and regarding the size, may not suit to many applications. Hence, to improve different system performances the demand for wideband compact planar EBG operating at lower bands is highly noticeable.

A planar via less EBG configuration with smaller unit cell is proposed here that exhibits a wide band gap at lower

frequency bands below 6 GHz. The band gap is analyzed with different parameter variation and finally enhanced by incorporating meander-line bridges. The proposed design is very simple and compact and can easily be integrated with the low frequency applications such as GSM, PCS, Bluetooth, Wi-Max, Wi-Fi etc.

Characteristics of the planar EBG structures

A schematic view of the proposed planar Jerusalem-Cross EBG (JC-EBG) unit cell is demonstrated in Figure 1(i) and an equivalent circuit model is conceptualized in Figure 1(ii). Since wide band gap at lower frequency ranges are much desirable, so the structure is aimed to operate at lower frequencies than 6 GHz. Several modifications have been done on the initial rectangular unit cell and one of the optimized shapes is demonstrated here.

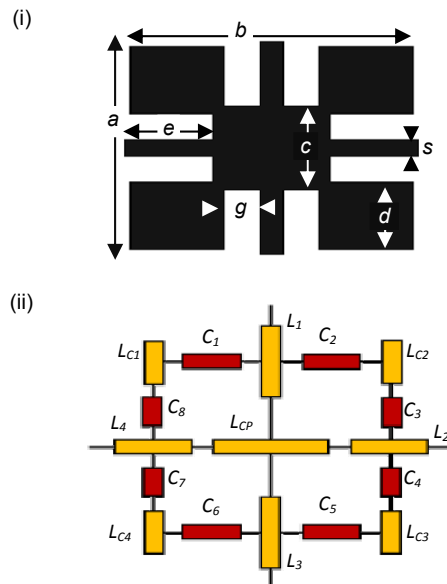


Fig. 1. (i) Schematic view of the JC-EBG unit cell (ii) Block representation of equivalent circuit model

The unit cell comprises of two different size patches and has a compact dimension of 12.5 x 12.5 mm². A square shape patch in placed at the center position which is connected to four other square metallic pads on the corner sides. Four narrow rectangular strips come out from the

central patch that established the connecting bridges with the adjacent patches. The whole metallic EBG pattern is etched on the top layer of a 0.508 mm dielectric substrate with permittivity=3.00 and loss tangent=0.013. The design parameters of the JC-EBG unit cell are as follows (all in mm):

$$a=12.5, b=12, c=6, d=5, e=3.75, g=2.5, s=1$$

In Figure 1(ii), the inductive and capacitive elements are represented by yellow and red blocks, respectively. The connecting bridges and the gaps contribute to the inductive (L_1, L_2, L_3 and L_4) and capacitive effect respectively. The inductances of the corner patches are indicated by Lc_1, Lc_2, Lc_3 and Lc_4 and $C_1, C_2, C_3, C_4, C_5, C_6, C_7$ and C_8 represent the internal capacitances created between the corner patches and the bridge lines. Moreover, some additional capacitances are formed between the gaps of any two adjacent cells. The integrated LC effect is the most important factor in determining the band gap of the EBG. Even though no particular relation is found to calculate the impedance nature of an EBG structure with non-uniform geometries, inductance (L) and capacitance (C) of a square shape ($W \times W$) EBG cell can be predicted by following relations [5,9].

$$(1) \quad L = \mu_0 \mu_r h$$

$$(2) \quad C = \varepsilon_0 (\varepsilon_r + 1) \frac{W + g}{\pi} \ln \left\{ \cos \frac{\pi g}{2(W + g)} \right\}$$

where: ε_0 – permittivity, μ_0 – permeability of free space, ε_r – relative permittivity, μ_r – relative permeability, g – gap width between adjacent cells, and h – thickness of the substrate.

And the center frequency of the EBG structure can be predicted by (3), also the width of the band gap by (4).

$$(3) \quad f = \frac{1}{2\pi\sqrt{LC}}$$

$$(4) \quad BW = \frac{1}{\eta} \sqrt{\frac{L}{C}}$$

Commercially available finite element method (FEM) based 3D full wave electromagnetic solver HFSS™ is utilized to design and simulate the proposed EBG structures. Initially, the JC-EBG performances are studied extensively and sequentially all the analysis is presented; after that the configuration is further modified and performances are examined. The bandwidth of the stop band (band gap) of the EBG structure with a finite number of unit cells is calculated by the directive transmission method [21]. The simulation model for the EBG is as shown in Figure 2. A two-port waveguide is used and the EBG structure is kept inside the waveguide. The wave ports are assigned along Y-axis. A pair of boundary walls of the waveguide is considered as perfect magnetic conductor (PMC) and the other pair is as perfect electric conductor (PEC). From each port incident waves are launched into the free space of the waveguide. The reflection and transmission characteristics through the waveguide are analyzed and the band gap is computed.

Figure 3 depicts the frequency response of the JCEBG structure and fractional bandwidth with respect to center frequency; in terms of variation of bridge width (s), central patch (c) and corner patch width (d). It can be seen from Figure 3(i)-(ii) that when the bridge width s increases, wider

band gap is resulted but the center frequency gradually shifted to the higher frequency. When $s = 0.25$ mm, the center frequency of the EBG is at 3.6 GHz and maximum bandwidth obtained is 79.2%. However, a decreasing trend of bandwidth is observed with increased bridge width, beyond $s = 0.25$ mm. For the second case of central patch size (c) variation, shifting of the band gap is noticed with larger patch size even though the bandwidth is remained almost same.

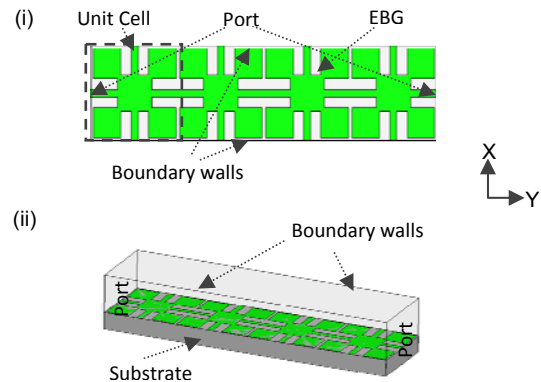


Fig.2. Simulation model of directive transmission method

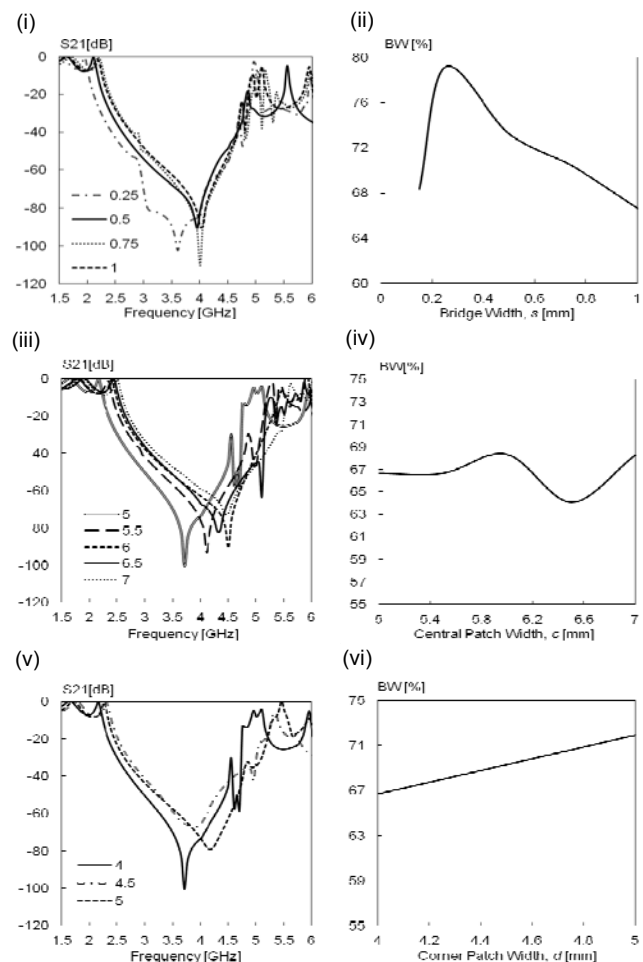


Fig. 3. (i), (iii), (v) Frequency response and (ii), (iv), (vi) Fractional bandwidth with respect to bridge width, central patch and corner patch width variation, respectively.

The responses are shown in Figure 3 (iii)-(iv). In both cases, the minimum transmission coefficient (S_{21}) level is around -90 dB to -110 dB. Similarly, it can be seen from Figure 3(v)-(vi) that when the corner patches (d) are enlarged, the band gap and center frequency shifted to the

higher band. However, the minimum level of S_{21} is higher than that with smaller corner patch, though slight improvement in band gap is observed. In all cases, above the frequency about 5 GHz, the structure showed some fluctuation in frequency responses. Eventually, a stop band results from the individual response of a unit cell and the collective response of the EBG array, which in turn provide a wide band gap. Due to this, several narrow stop band resonances are observed above 5 GHz which are close to each other but not overlapped. As this study concerned to obtain a wide band gap for below 6 GHz frequency bands, those resonances are not tuned further which may affect the provided results otherwise. The reasons behind the band shifting and widening is the variation of the capacitive and inductive effects with respect to the design parameters (s , d , and c) variation. The size adaptation of the central and corner patches affect the internal gap capacitances (C_1, C_2, \dots, C_8) and their self inductances ($L_{C1}, L_{C2}, \dots, L_{C4}$); and the bridge inductances (L_1, L_2, \dots, L_4) are controlled by the bridge length and width.

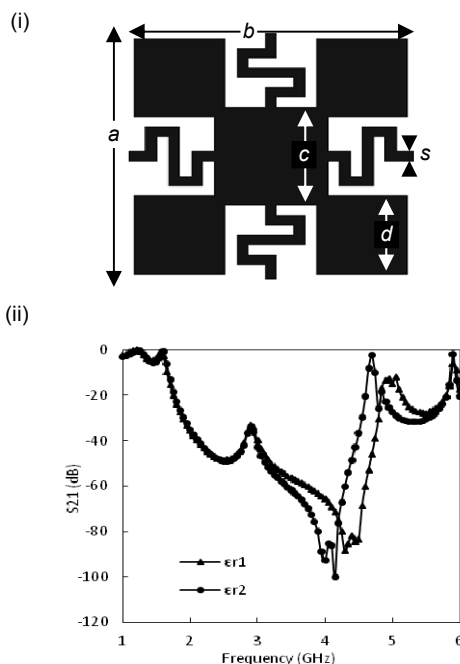


Fig. 4. (i) Schematic view of the modified JC-EBG unit cell (ii) Frequency response with two different substrates.

Based on the aforesaid design analysis, the initial JC-EBG design is modified as shown Figure 4(i). The straight bridges are substituted by the meander lines in order to enhance the performance by lengthening the connecting path while the overall cell size is remained unchanged. The parameters are carefully chosen to maintain the wide band gap and lowest possible level of S_{21} . By reducing the bridge width (s) to 0.5 mm, the effective length of the bridge is increased to 8.75 mm. The ratio of length to width of the new bridge is become 17.5, while it was only 3.75 mm for the previous one and the inductances of the connecting bridges (L_1, L_2, L_3 and L_4) become higher as well. These additional inductive effects contribute to total impedance and the whole EBG pattern provides higher surface impedance than the previous configuration.

With the optimal parameters, the modified configuration is designed, simulated and analyzed by HFSS. In order to see the stability of the band gap at lower frequency region, the frequency responses of the new pattern are computed with two different substrate materials of the same thickness (0.508 mm) consecutively and results are shown in Figure

4(ii). To observe the performance improvement, the modified design is considered on the same substrate used before ($\epsilon_r1=3.00$, $\tan\delta=0.013$). The band gap achieved is 3.1 GHz that covers the lower bands from 1.75 GHz to 4.85 GHz and the lowest value of S_{21} is around -90 dB. With another substrate ($\epsilon_r1=3.38$, $\tan\delta=0.027$) the band gap achieved is 2.8 GHz (24.44%) covering 1.75 to 4.55 GHz. For both substrates the band gap characteristics are quite similar, remained in the lower range; but the previous bandwidth is still better. However, due to the design modification with meander line bridges, the impedance is increased and hence the new structure showed 31.91% much wider band gap and deeper level of the transmission coefficient than the initial one. Needless to mention that wide band gap with a minimum value of S_{21} is highly expected characteristics of an artificially designed periodic structure like EBG, so that it can suppress or restrict the propagation of surface waves well enough for the desired band.

To verify the HFSS simulated transmission characteristics, the modified JC-EBG structure is modelled and simulated using another well-known electromagnetic solver CST microwave studio. The HFSS is a finite element method (FEM) based solver whereas the CST is a frequency division time domain (FDTD) based simulator. Figure 5 shows the frequency responses obtained from these two different simulators. The achieved band gaps for HFSS and CST simulations are 2.3 GHz (1.75-4.85 GHz) and 2.1 GHz (2.65-4.75 GHz) respectively. Comparing the HFSS and CST simulated results, good co-relation is found except a slight decrease in the band gap range and the minimum rejection (S_{21}) level.

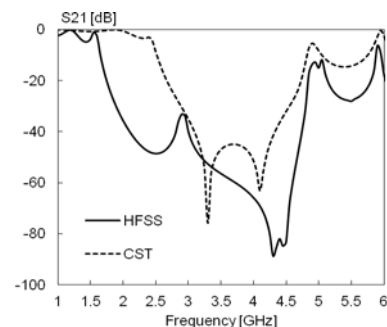


Fig. 5. Frequency responses of the modified JC-EBG structure obtained from CST and HFSS

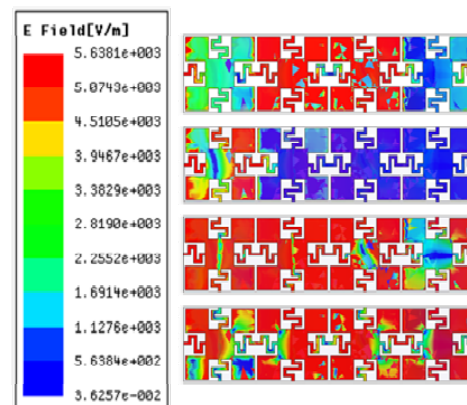


Fig. 6. E-field distribution of the new unit cell at 1.5, 4.3, 5.0 and 5.9 GHz (top to bottom, respectively).

Figure 6 elucidates the electric field distribution of the modified JC-EBG at different frequencies. At the frequencies outside the band gap (1.5, 5 and 5.9 GHz) the

transmission is occurred, though it is not allowed inside the band gap at 4.3 GHz. The EBG exhibits blocking property for the waves within the band gap only, otherwise the transmission is occurred.

Table 1. Performance comparison of the both EBG structures.

	JC-EBG	Modified JC-EBG
UC size	12.5 mm	12.5 mm
-10 dB BW	2.65 GHz	3.3 GHz
-20 dB BW	2.35 GHz	3.1 GHz
-30 dB BW	2.25 GHz	2.65 GHz
-20 dB BW	66.67%	93.94%
S_{21} Level	-100 dB	-90 dB

The results obtained with JC-EBG and modified JC-EBG is summarized in Table I for easy comparison and better understanding. All the analysis on the proposed EBG structure proves the existence of the wide band gap at lower frequency bands, despite of its compactness. Without increasing the cell size a tradeoff among the design parameters is considered to obtain the best possible result. So, considering the wide application range in lower bands the proposed compact configuration is suitable for various applications such as GSM, PCS, Bluetooth, Wi-Max, Wi-Fi etc.

Conclusions

In this study, two compact designs of planar EBG with wide band gap are studied and their performances are compared. Varying only one design parameter while other parameters and overall size are kept unchanged, significant improvement is observed. Insertion of meander line bridges instead of straight line enhanced the EBG performances in terms of band gap and transmission coefficient value. The band gap achieved with initial design is 2.35 GHz (66.67%), and with the final design is 3.1 GHz (93.94%). Within the targeted frequency ranges (<6 GHz), the lowest transmission level is around -100 dB and thus can increase system's functionality by suppressing unwanted wave propagation. The proposed EBG showed selectivity and tunability for the desired lower band. For a remarkable number application operates within these bands, this design can be a perfect choice to integrate with the systems.

REFERENCES

[1] Park Y.J., Herschlein A., and Wiesbeck W., A photonic bandgap (PBG) structure for guiding and suppressing surface waves in millimeter-wave antennas, *IEEE Transactions on Microwave Theory and Techniques*, 49(2001), nr 10, 1854-1859.

[2] Mobashsher, A.T., Islam, M.T., and Misran, N., A novel high-gain dual-band antenna for RFID reader applications. *IEEE Antennas and Wireless Propagation Letters*, 9 (2010), 653-656.

[3] Azim, R., Islam, M.T., and Misran, N., Ground modified double-sided printed UWB antenna. *Electronics Letters*, 47(2011), nr. 1, 9-10.

[4] Alam, M.S., and Islam, M.T., Design of high impedance electromagnetic surfaces for mutual coupling reduction in patch antenna array. *Materials*, 6(2013), nr. 1, 143-155.

[5] Sievenpiper D., Zhang L., Broas R.F.J., Alexopolous N.G., and Yablonovitch E., High impedance electromagnetic surfaces

with a forbidden frequency band, *IEEE Trans. Microw. Theo. Tech.*, 47(1999), nr 11, 2059-2074.

[6] Azim, R., Islam, M.T., and Misran, N., Planar UWB antenna with multi-slotted ground plane. *Microwave and Optical Technology Letters*, 53(2011), nr. 5, 966-988.

[7] Broas R.F.J., Sievenpiper D.F., and Yablonovitch E., A high-impedance ground plane applied to a cell-phone handset geometry, *IEEE Trans. Microw. Theo. Tech.*, 49(2001), nr 7, 1262-1265.

[8] Assimonis S.D., Yioultis T.V., and Antonopoulos C.S., Computational investigation and design of planar EBG structures for coupling reduction in antenna applications, *IEEE Transactions on Magnetics*, 48(2012), nr 2, 771-774.

[9] Alam, M.S., Islam, M.T., and Misran, N., A novel compact split ring slotted electromagnetic bandgap structure for microstrip patch antenna performance enhancement, *Progress in Electromagnetics Research*, PIER 130(2012), 389-409.

[10] Yang F., and Rahmat-Samii Y., Electromagnetic band gap structures in antenna engineering, *Cambridge University Press*, 2009.

[11] Shahparnia S. and Ramahi O.M., Electromagnetic interference (EMI) reduction from printed circuit boards (PCB) using electromagnetic bandgap structures, *IEEE Transactions on Electromagnetic Compatibility*, 46(2004), 580-587.

[12] Alam, M.S., Islam, M.T., and Misran, N., Inverse triangular shape CPW-fed antenna loaded with EBG reflector, *Electronics Letters*, 49(2013), nr. 2, 86-88.

[13] Yang F., and Rahmat-Samii Y., Microstrip antennas integrated with electromagnetic band-gap structures: a low mutual coupling design for array applications, *IEEE Transactions on Antennas and Propagation*, 51(2003), 2936-2946.

[14] Mosallaei H., and Sarabandi K., A compact wide-band EBG structure utilizing embedded resonant circuits, *IEEE Antennas and Wireless Propagation Letters*, 4(2005), 5-8.

[15] Abedin M.F., and Ali M., Effects of a smaller unit cell planar EBG structure on the mutual coupling of a printed dipole array, *IEEE Antennas and Wireless Propagation Letters*, 4(2005), 274-276.

[16] Raimopno L., Paulis F.D., and Orlandi A., A simple and efficient design procedure for planar electromagnetic bandgap structures on printed circuit boards, *IEEE Transactions on Electromagnetic Compatibility*, 53(2011), nr 2, 482-490.

[17] Coccioli R., Yang F.R., Ma K.P., and Itoh T., Aperture-coupled patch antenna on UC-PBG substrate, *IEEE Trans. Microw. Theo. Tech.*, 47(1999), 2123-2130.

[18] Rahman M. and Stuchly M., Wide-band microstrip patch antenna with planar PBG structure, *Proceedings of the IEEE AP-S International Symposium Digest*, 2(2001), 486-489.

[19] Abedin M.F., Azad M.Z., and Ali M., Wideband smaller unit-cell planar EBG structures and their application, *IEEE Transactions on Antennas and Propagation*, 56(2008), nr 3, 274-276.

[20] Kwak S.I., Sim D.U., and Kwon J.H., Design of optimized multilayer PIFA with the EBG structure for SAR reduction in mobile applications, *IEEE Transactions on Electromagnetic Compatibility*, 53(2011), nr 2, 325-331.

[21] Liang L., Liang C.H., Chen L., and Chen X., A novel broadband EBG using cascaded Mushroom-like structure, *Microwave and Optical Technology Letters*, 50(2008), nr 8, 2167-2170.

Authors: Mr. Md. Shahidul Alam, Prof. Dr. Mohammad Tariqul Islam, and Prof. Dr. Norbahiah Misran are with the Department of Electrical, Electronic & Systems Engineering, and the Institute of Space Science (ANGKASA), Universiti Kebangsaan Malaysia, 43600 Bangi, Selangor, Malaysia, E-mails: titu_jfc@yahoo.com, titareq@yahoo.com, bahiah@eng.ukm.my.